

Article

# A Process Study of Seiches over Coastal Waters of Shenzhen China after the Passage of Typhoons

Guotong Deng <sup>1</sup>, Jiuxing Xing <sup>1</sup>, Jinyu Sheng <sup>1,2</sup> and Shengli Chen <sup>1,\*</sup>

<sup>1</sup> Institute for Ocean Engineering, Shenzhen International Graduate School, Tsinghua University, Shenzhen 518055, China; dgt18@mails.tsinghua.edu.cn (G.D.); jxx2012@sz.tsinghua.edu.cn (J.X.); jinyu.sheng@dal.ca (J.S.)

<sup>2</sup> Department of Oceanography, Dalhousie University, Halifax, NS B3H 4R2, Canada

\* Correspondence: shenglichen@sz.tsinghua.edu.cn

**Abstract:** Analysis of sea-level observations demonstrates that Typhoons Mawar (2017) and Mangkhut (2018) induced seiches in both Dapeng Bay and Daya Bay near Shenzhen of China, with periods varying from about 3.5 to 4.0 h. Typhoon Mawar (2017) also generated seiches with a period of about 1.2 h. Seiches with such periods in the two bays have not been reported in the past. In this study, we investigate the main processes affecting seiches over these coastal waters using a nested-grid ocean circulation modeling system. The modelled results of typhoon-induced seiches agree well with observations, which indicates that the seiches after the passage of typhoons are dynamically free waves generated by the storm-induced accumulation of water bodies in the two bays. Model sensitivity experiments show that wind directions have an important influence on the type and characteristics of seiches. When the wind stress causes the water body to accumulate in a cross-bay direction, seiches in a closed water body are generated. When the wind stress causes the water body to accumulate in an along-bay direction, seiches in a semi-closed water body are produced. Because of the irregularity of the bathymetry and coastline and variability of wind directions, these two types of seiches can exist simultaneously in the two bays.



**Citation:** Deng, G.; Xing, J.; Sheng, J.; Chen, S. A Process Study of Seiches over Coastal Waters of Shenzhen China after the Passage of Typhoons. *J. Mar. Sci. Eng.* **2022**, *10*, 327. <https://doi.org/10.3390/jmse10030327>

Academic Editor: Rafael J. Bergillos

Received: 17 January 2022

Accepted: 22 February 2022

Published: 25 February 2022

**Publisher's Note:** MDPI stays neutral with regard to jurisdictional claims in published maps and institutional affiliations.



**Copyright:** © 2022 by the authors. Licensee MDPI, Basel, Switzerland. This article is an open access article distributed under the terms and conditions of the Creative Commons Attribution (CC BY) license (<https://creativecommons.org/licenses/by/4.0/>).

**Keywords:** seiches; typhoon; Shenzhen; ocean model; topography; coastal waters

## 1. Introduction

Seiches are oscillations in a closed or semi-closed water body, such as lakes or coastal bays [1]. Their periods are the local natural resonance periods for the water body, depending on the geometry of the shoreline and the bathymetry [2]. The amplitude of seiches can reach about 45 cm in the coastal waters off Shenzhen, China [3]. For effective protection of human and economic activities over coastal areas with small tidal ranges, such as Dapeng Bay near Shenzhen (an important economic and shipping center in China [4]), close attention should be paid to the influence of seiches over these areas.

In a lake or a coastal embayment, when winds (or other external forces, such as atmospheric pressure perturbances) contain the oscillation of the natural frequencies of the water body, even if the wind forcing is very weak, significant “free” oscillations of sea levels can be generated [5]. In addition, when the movement of the wind forcing meets the resonant characteristics of the water body, the response of the water body will be amplified. Seiches are difficult to replicate over coastal regions because there is no physical boundary on the shelf side of a bay to block the outflow and reflect the undulation of the water surface [6]. Seiches can be triggered, however, by winds (or atmospheric pressure perturbations) relatively easily in bays with particular bathymetry and coastal orography, such as the Adriatic Sea [7]. The amplitudes of seiches were found to exceed 1.0 m over some coastal waters, such as 0.5 to 1.0 m at Ciutadella in the western Mediterranean with the maximum amplitude of about 1.5 m [8], and about 1.8 m at the Neuse River Estuary in the United States [9].

Chuang and Boicourt [6] studied seiches in Chesapeake Bay of the United States. They found that seiches in the bay with periods from 2 to 3 days are induced by the north-southerly winds, and seiches induced by the east-westerly winds have a period of 1.6 days. Since ocean currents driven by the east-westerly winds occurred only at the mouth of the Bay, Chuang and Boicourt [6] suggested that it is the wind forcing in the bay mouth that triggers the seiches of the entire bay. Gomis et al. [8] examined seiches around the Balearic Islands and found that the oscillation of the sea level is significantly related to the change of atmospheric pressures. Their study demonstrated that the seiches are not generated by the atmospheric disturbances directly but by sea-level fluctuations caused by wind forcing, and these sea-level fluctuations are in an inverse phase with atmospheric disturbances. Lemon [10] investigated the correlation between the amplitude of seiches and edge waves in Port San Juan and found that the seiches in the port are intermittent and short-lived, not significantly correlated with astronomical tides and storm surges. Lemon [10] suggested that the seiches in Port San Juan are most likely generated by long periodic fluctuations in the open sea.

For the coastal waters of China, Fan and Xu [11] found that seiches in a coastal bay, known as Laohutan of Dalian City, are not directly related to atmospheric forcing, ocean waves and other factors, but to the displacement of the geological plate over the coastal sea near Laohutan. Cao et al. [12] analyzed seiches with amplitudes greater than 50 cm in the Bohai Sea and the Yellow Sea and found that most of the seiches with large amplitudes are related to thunderstorms. Li [4] analyzed seiches in Dapeng Bay off Shenzhen City of Guangdong Province and reported that seiches in the bay have amplitudes of about 10 cm, and sometimes reaches about 50 cm, and have periods between 20 and 50 min with a dominant period of 40 min. Wu et al. [3] compared seiches in Daya Bay off Shenzhen and Haizhou Bay off Lianyungang City of Jiangsu Province and argued that the amplitudes and periods of seiches in these two bays are significantly different. They suggested that the main reason for these differences may be due to different sizes, shapes and depths of the two bays, but they did not examine the influence of these factors on seiches in detail in the two bays.

Generations and characteristics of seiches differ significantly over different coastal waters. Most previous studies on seiches over coastal waters off Shenzhen focused mainly on periods and amplitudes of seiches without systematic investigations of the generation mechanisms and influencing factors of seiches. Based on sea-level observations in Daya Bay and Dapeng Bay, in this study, we analyze seiches after the passage of typhoons and investigate the generation and characteristics of seiches using a nested-grid modeling system based on the Regional Ocean Modeling System (ROMS) [13]. We also examine model results in idealized experiments using a wind pulse to determine different kinds of seiches, i.e., those with characteristics of both “closed water body” and “semi-closed water body”, coexist over the coastal waters off Shenzhen due to changes in wind directions.

The structure of this paper is as follows. Section 2 provides observations of seiches after Typhoons Mangkhut and Mawar and calculations of seiches in ideal basins. Section 3 describes the setup and validation of the modeling system. The mechanism of seiches in Dapeng and Daya Bays is investigated in Section 4, and a summary is given in Section 5.

## 2. Observations and Theoretical Calculations of Seiches

### 2.1. Observations of Seiches

The main study area of this paper is Dapeng Bay, Daya Bay and adjacent coastal waters off Shenzhen. Dapeng Bay is located at the junction of Shenzhen and Hong Kong and is a semi-enclosed bay with many islands to the west. Daya Bay is also a semi-enclosed bay with several smaller bays inside (see Figure 1).

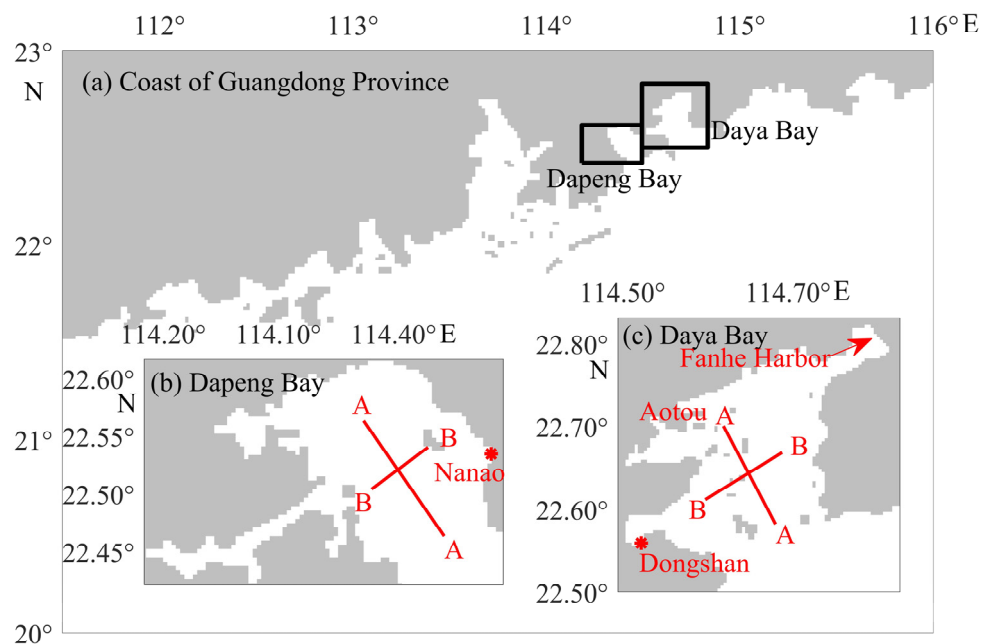


**Figure 1.** (a) Coastline of Guangdong Province of China, (b) Dapeng Bay and (c) Daya Bay off Shenzhen City and positions of Nanao and Dongshan stations. The A–A direction is the along-bay direction, and the B–B direction is the cross-bay direction.

Sea level measurements at stations Nanao in Dapeng Bay and Dongshan in Daya Bay off Shenzhen during and after the passages of Typhoons Mangkhut and Mawar are used in this study to determine the observed characteristics of seiches over coastal bays off Shenzhen. Station Nanao is located in the eastern Dapeng Bay (Figure 1b), and station Dongshan is located in the southwestern Daya Bay (Figure 1c) off Shenzhen. The observational sea level data were obtained from the Shenzhen Marine Monitoring and Forecasting Center.

Typhoon Mawar made landfall in eastern Shenzhen at 13:30 UTC on 3 September in 2017 with a maximum wind speed of about 56 m/s. Typhoon Mangkhut made landfall in western Shenzhen at 09: 00 UTC on 16 September in 2018 with an estimated maximum sustained wind speed of about 69 m/s.

The power spectrum analysis was carried out using the observed 10-min sea levels made at the two stations during a two-day period right after the passage of the typhoon. The tidal components were removed before the spectral analysis. The analysis results at these two stations are shown in Figures 2 and 3.

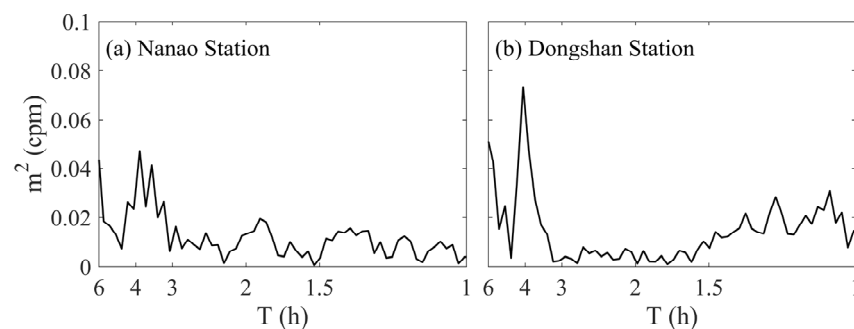


**Figure 2.** Power spectra of observed 10-min sea levels with tidal components removed at (a) Nanao and (b) Dongshan stations after the passage of Typhoon Mangkhut in September 2018.

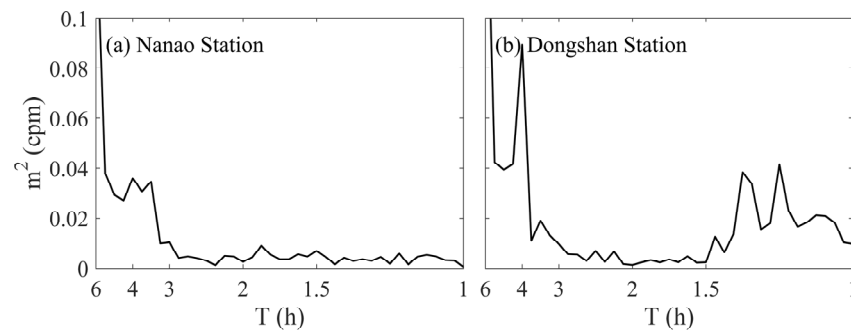


**Figure 3.** Power spectra of observed 10-min sea levels with tidal components removed at (a) Nanao and (b) Dongshan stations after the passage of Typhoon Mawar in September 2017.

Figure 2 demonstrates that, after Typhoon Mangkhut, the observed 10-min sea levels at the two stations had significant free oscillations (seiches). The period for the highest peak in the power spectrum is about 3.8 h at Nanao in Dapeng Bay (Figure 2a) and about 4.0 h at Dongshan in Daya Bay (Figure 2b), with an oscillation amplitude of about 20 cm at Nanao and 27 cm at Dongshan. After Typhoon Mawar, the period for the highest peak in the power spectrum is about 3.5 h at Nanao (Figure 3a) and 4.0 h at Dongshan (Figure 3b), with an amplitude of about 19 cm at Nanao and 30 cm at Dongshan. Furthermore, there were seiches with a period of about 1.2 h and an amplitude of 20 cm at Dongshan in Daya Bay (Figure 3b). As to be discussed later, a typhoon of the same intensity but with a different landfall position can lead to different wind forcing and different patterns of sea level setup in a bay and, therefore, generate different types of seiches.

Previous studies based on sea-level observations from May to October 1985 in Dapeng Bay demonstrated that periods of primary seiches in the bay varied from 0.3 to 1.0 h, with a dominant period of about 0.7 h [4]. The period of primary seiches in Daya Bay caused by typhoons (8607, 8613 and 8616) was found to be about 1.2 h [3]. Our literature review shows that seiches with a period of about 4.0 h have not been reported before. The causes for differences in periods of seiches in these bays need to be further investigated.

### 2.2. Theoretical Consideration

As mentioned in the introduction, seiches are standing oscillations with different modes in an enclosed or semi-enclosed basin or in a locally isolated part of a basin, and these dynamically free oscillations occur at the natural resonant periods of the basin [2]. The natural resonant periods of oscillations in a narrow basin or channel (1D) can be calculated by Merian’s formula [14]. For a semi-closed channel (i.e., a channel with one open end and one closed end) with a constant water depth ( $h$ ), such as a coastal bay, the natural periods can be computed based on:

$$T_n = \frac{4L}{(2n - 1)\sqrt{gh}}, n = 1, 2, 3, \dots, \tag{1}$$

For a closed narrow channel, such as an elongated lake, the natural periods are given as:

$$T_n = \frac{2L}{n\sqrt{gh}}, n = 1, 2, 3, \dots, \tag{2}$$

In the above equations  $T_n$  represents the period in the  $n$ th mode of seiches,  $L$  the length of the channel,  $h$  the water depth and  $g$  the earth’s gravitational acceleration. If a basin is not narrow (2D), such as a rectangular basin with length  $L$  and width  $l$ , the natural periods are given as [15]:

$$T_{mn} = \frac{2}{\sqrt{gh}} \left[ \left( \frac{m}{L} \right)^2 + \left( \frac{n}{l} \right)^2 \right]^{-1/2}, m, n = 0, 1, 2, 3, \dots, \tag{3}$$

where  $m$  and  $n$  are the node numbers in  $L$  and  $l$  directions. For a semi-closed rectangular (2D) basin, however, theoretical periods cannot be derived readily. Expressions for natural periods of seiches in other idealized basins can be found in the review paper by Rabinovich [2].

The bathymetry and coastline of Dapeng and Daya Bays are complicated. In order to study the influence of wind directions on seiches, these two bays are approximated as one-dimensional channels along and across the mouth of the bay for the simplicity of discussions here. As Dapeng and Daya Bays are approximated as one-dimensional channels, they can be regarded as semi-closed water bodies in the along-bay direction (A–A direction) and closed water bodies in the cross-bay direction (B–B direction) (Figure 1).

For seiches in these two bays, we calculate the natural periods in the two directions of the first three modes using Equations (1) and (2). The higher modes of seiches are not considered here due to their low energy levels. Our calculation results are shown in Table 1. The primary periods of the observed seiches after Typhoons Mangkhut and Mawar are close to the periods of the first mode of seiches in a semi-closed water body. The primary period of observed seiches caused by Typhoon Mawar in Daya Bay is close to the period of the second mode in a semi-closed water body or the first mode in a closed water body, which is close to previous estimations made on observations in the literature [3]. This suggests that the dynamically-free oscillations generated by different typhoons can be two or more different types and characteristics of seiches in the two bays. Landing paths of various typhoons are very different, which can be the main cause for different patterns of sea level setup and, therefore, different types of seiches.

**Table 1.** Estimated natural periods of Dapeng and Daya Bays based on Equations (1) and (2).

	Natural Periods (Hours)	
	Dapeng Bay	Daya Bay
$L$ (km) in A–A direction	25.0	25.0
$L$ (km) in B–B direction	14.0	18.0
$h$ (m)	8.5	6.3
$T_1$ (hours) in A–A direction	3.0	3.5
$T_1$ (hours) in B–B direction	0.9	1.3
$T_2$ (hours) in A–A direction	1.0	1.2
$T_2$ (hours) in B–B direction	0.4	0.6
$T_3$ (hours) in A–A direction	0.6	0.7
$T_3$ (hours) in B–B direction	0.3	0.4

### 3. Model Setup and Validation

A nested-grid ocean circulation modeling system is used in this study to improve our understanding of the generation and propagation of seiches in Dapeng and Daya Bays. The modeling system is based on the Regional Ocean Modeling System (ROMS), which uses a terrain-following coordinate in the vertical [16] for the 3D setup.

The nested-grid modeling system has three sub-models: a course-resolution outer sub-model, an intermediate-resolution middle sub-model and a fine-resolution inner sub-model (Figure 4). Since the two typhoons considered in this study swept the northern South China Sea, the domain of the outer sub-model, therefore, covers the northern South China Sea, ocean waters around Taiwan and northern China Sea, with a horizontal resolution of about 9.0 km. The domain of the middle sub-model covers the coastal and shelf waters of Guangdong with a resolution of about 1.8 km. The domain of the inner sub-model covers the main study area of this paper: the coastal waters off Shenzhen, with a resolution of about 400 m.

In this study, only the barotropic dynamics in response to atmospheric forcing (i.e., wind forcing and atmospheric pressure perturbations) and tidal forcing are considered for simplicity. The outer and middle sub-models are two-dimensional, and the inner sub-model is three-dimensional with 10 vertical sigma layers. The inner sub-model utilizes time-splitting

methods to treat internal and external modes separately, and the time interval of the external mode is 25, 5 and 2 s, respectively, and the time interval of the internal mode of the model is 40 s.

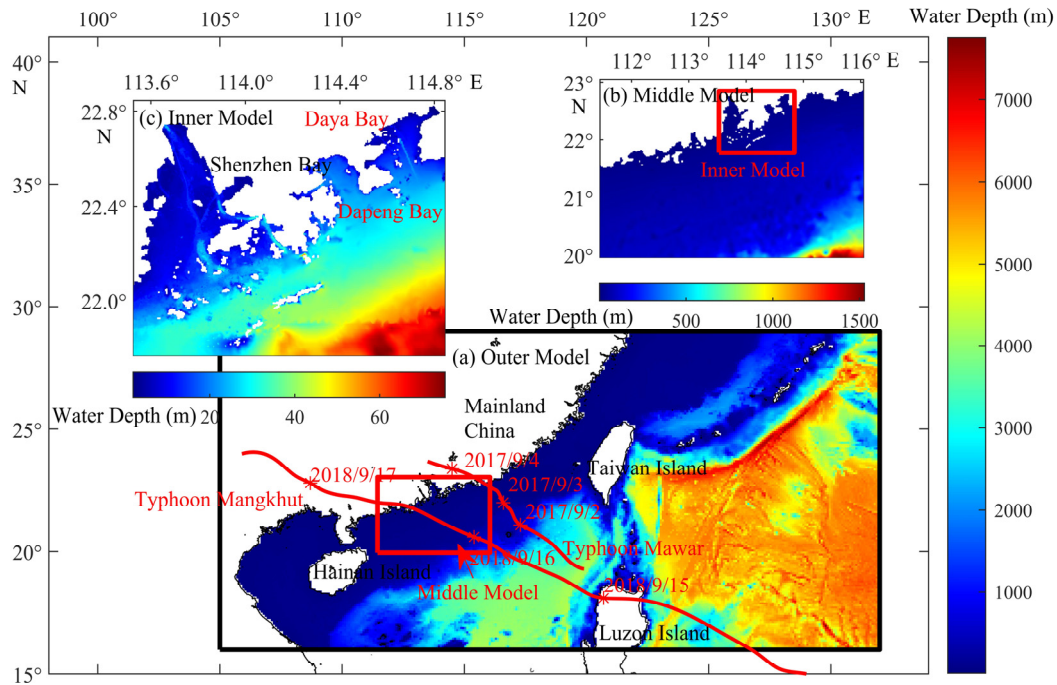


**Figure 4.** Major topographic features over domains of (a) the outer model, (b) middle model and (c) inner model of the nested-grid ocean circulation modeling system.

Unstructured grid ocean models, such as FVCOM (e.g., [17]), utilize variable size grids to have the advantage of having fine horizontal resolutions over areas of interest. In a separate work, the FVCOM was applied to the same study area with a near-shore horizontal resolution of the order of 10. Both models based on FVCOM and ROMS give similar results.

The hurricane model developed by Holland [18] is used for the wind and the atmospheric pressure perturbations at the mean sea level associated with a typhoon based on

$$V(r) = \left\{ \frac{B}{\rho_a} \left( \frac{R}{r} \right)^B \left( (P_\infty - P_0) \exp \left[ - \left( \frac{R}{r} \right)^B \right] + \left( \frac{rf}{2} \right)^2 \right) \right\}^{0.5} - \frac{rf}{2}, \quad (4)$$

$$p(r) = P_0 + (P_0 - P_\infty) \left( - \frac{R}{r} \right)^B, \quad (5)$$

where  $V(r)$  is the wind speed and  $p(r)$  is the air pressure;  $P_\infty$  and  $P_0$  are the typhoon’s peripheral pressure and central pressure, respectively;  $r$  is the distance from the calculation point to the typhoon center;  $R$  is the radius of maximum wind speed;  $f$  is the Coriolis parameter;  $\rho_a$  is the air density; and  $B$  is the Holland fitting parameter. The data for the path and atmospheric pressures at the center of the typhoon used in this study were extracted from the CMA Optimal path dataset of the Tropical Cyclone Data Center of China Meteorological Administration [19,20]. The tidal forcing is specified at the open boundaries of the modeling system based on results produced by the global ocean tide model TPX09 [21].

The nested-grid modeling system is used to simulate sea levels and three-dimensional (3D) currents over coastal waters off Shenzhen before, during and after the passage of Typhoon Mangkhut. The model output interval is set at 10 min as the same as the observations. Figure 5 presents time series of observed and simulated sea levels at Nanao

and Dongshan stations during the period from 9 to 18 September 2018. The simulated sea levels agree very well with the measured values at these two stations. The root mean square error (RMSE) for the results produced by the inner sub-model is about 0.27 m at these two stations. The correlation coefficients (R) are about 0.88 at Nanao and 0.89 at Dongshan. In addition, the inner sub-model reproduces the observed storm surge induced by Typhoon Mangkhut reasonably well, with a model error of less than 10% for simulating the maximum sea level.

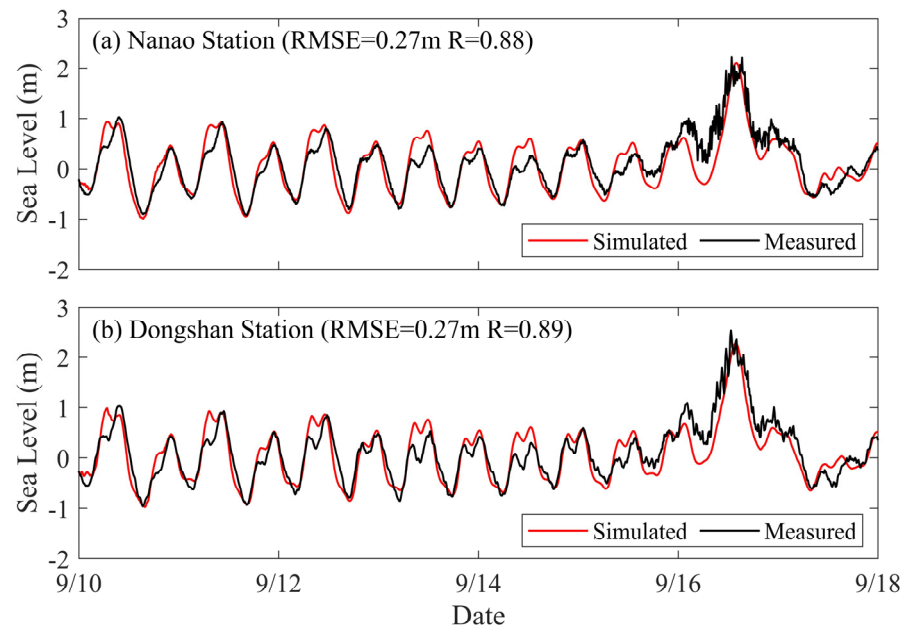


**Figure 5.** Time series of observed and simulated sea levels at stations (a) Nanao in Dapeng Bay and (b) Dongshan in Daya Bay. The storm center of Typhoon Mangkhut passed these two stations at 09:00 UTC on 16 September 2018.

#### 4. The Mechanism of Seiches in Dapeng and Daya Bays

The nested-grid modeling system is used in this section to examine the main processes affecting the generation and propagation of seiches associated with Typhoon Mangkhut in Dapeng and Daya Bays off Shenzhen.

##### 4.1. Seiches after the Passage of Typhoons

Power spectrum analysis was first conducted for the time series of sea levels at 12 locations taken from results produced by the inner sub-model for two days between 02:00 UTC on 17 September and 02:00 UTC on 19 September 2018 after the passage of Mangkhut. These 12 locations include 6 locations in Dapeng Bay and 6 locations in Daya Bay off Shenzhen (Figure 6). The main reason for choosing these 12 locations is that they can reflect the difference of seiches in different parts of the bay.

The power spectra of simulated sea levels after the passage of Mangkhut have major peaks around the period of 3.6 h at the six locations in Dapeng Bay (Figure 7a) and around the period of 4.0 h at the six locations in Daya Bay (Figure 7b). The periods for major oscillations estimated from simulated sea levels agree reasonably well with periods for major seiches estimated from the observed sea levels, which are about 3.8 h in Dapeng Bay and about 4.0 h in Daya Bay (Figure 2). Figure 7a also demonstrates that the major oscillations produced in the inner sub-model have amplitudes between 15 and 20 cm at the six locations in Dapeng Bay, with a mean amplitude of about 17 cm. In Daya Bay, the amplitudes of major free oscillations are between 17 and 24 cm at the six locations, with a mean amplitude of about 20 cm. The estimated amplitudes of major oscillations based on simulated sea levels also agree with the observations, which are about 19 cm in Dapeng Bay and 30 cm in Daya Bay.

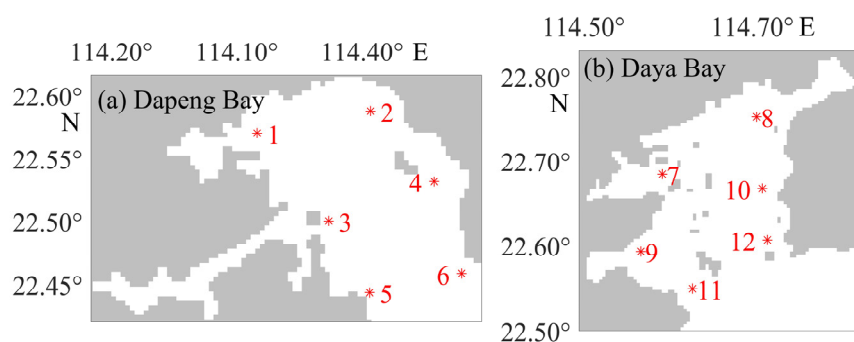


**Figure 6.** Positions of (a) the six locations in Dapeng Bay and (b) the six locations in Daya Bay (marked by numbers in red) off Shenzhen, Guangdong Province of China.

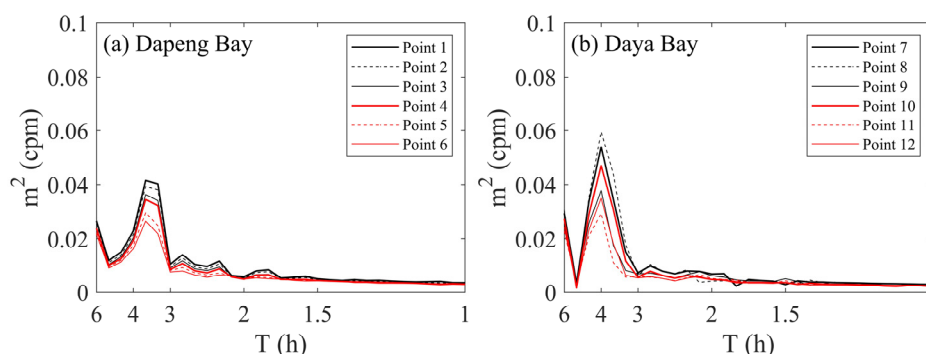


**Figure 7.** Power spectra of simulated sea levels at (a) the six locations in Dapeng Bay and (b) the six locations in Daya Bay based on results produced by the inner sub-model in the two-day period between 02:00 UTC on 17 September and 02:00 UTC on 19 September after Typhoon Mangkhut.

To examine the main characteristics of dynamically free oscillations after the passage of Typhoon Mangkhut, we consider the simulated sea levels in Daya Bay on 16 September after the passage of the Typhoon (Figure 8), based on results produced by the inner sub-model without tidal forcing.

At 14:00 on 16 September, about 5 h after the landfall of Mangkhut, a significant storm-induced setup occurred in Daya Bay (Figure 8a). The simulated sea levels in Daya Bay at this time vary from the maximum sea levels of about 25 cm at the head near Aotou and Fanhe Harbor to values of about 18 cm at the mouth of the bay. The sea levels in the bay decrease with time and are about 16 cm at the head near Aotou and about 8 cm at the mouth of the bay at 15:00 (Figure 8b). The simulated sea levels are near uniform and about 6 cm at the head and about 8 cm at the mouth of the bay at 16:00 (Figure 8c). In subsequent times, the simulated sea levels in the bay have free oscillations with one antinode (or node) at any given time, in the same way as the first mode of quarter-wave seiches in a semi-closed narrow channel with one open end [2,14].

It should be noted that many physical processes can generate seiches over coastal waters, such as wind stress, atmospheric pressure perturbations, onshore propagations of sea level perturbations from deep offshore waters, deep-sea internal waves and seismic activity. Our model results demonstrate that the seiches in the coastal bays off Shenzhen after the passage of Typhoon Mangkhut are the free oscillations induced by the relaxation of storm-induced sea level setup/setdown. These oscillations are the resonance motions of dynamically free waves. Therefore, wind directions should play a very important role in generating storm-induced setup and seiches over coastal waters because different wind directions can lead to the accumulation of water bodies in different regions in the bay, and hence affect the directions of free oscillation and periods of seiches.

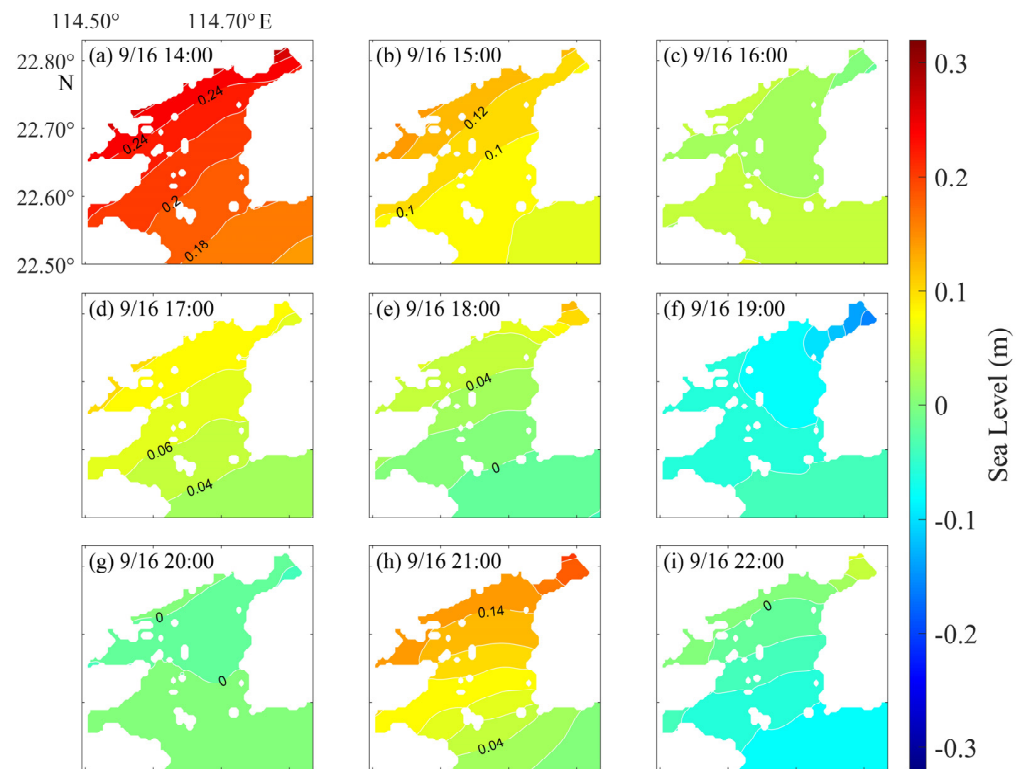


**Figure 8.** Distributions of instantaneous sea levels produced by the inner sub-model in Daya Bay at nine different times (a–i) between 14:00 and 22:00 on 16 September 2018 after the passage of Mangkhut.

#### 4.2. Effect of Wind Directions on Seiches

Typhoon Mangkhut made landfall in western Shenzhen. However, a typhoon in the future can make landfall at a different location with a different storm track, both of which can lead to different wind directions and intensities over coastal waters off Shenzhen. To investigate influences of wind directions on seiches in Dapeng and Daya Bays, four idealized numerical experiments were conducted using the same nested-grid modeling system but with a wind pulse. The main differences among these four idealized experiments are different directions of constant winds on the first day (F–D, E–C, D–F and C–E), as shown in Figure 9. The F–D axis is roughly in the across-bay direction of these two bays, and the C–E axis is roughly in the along-bay direction. The wind direction is parallel to the direction from point F to point D in case F–D, from point E to point C in case E–C and so on. In each idealized experiment, a wind pulse defined as a constant wind forcing on the first day (Table 2) and no wind forcing afterwards, is used to drive the nested-grid modeling system. The model is integrated for nine days in each idealized experiment. The model’s results produced by the inner sub-model in the four idealized experiments for two days right after the pulsing wind forcing are used to investigate seiches in the two bays off Shenzhen.

Power spectrum analysis was conducted for simulated sea levels at 12 locations in Dapeng and Daya Bays in each idealized experiment. These 12 locations are shown in Figure 6. A comparison of the model’s results among four idealized experiments demonstrates that seiches generated by the wind pulse in E–C and C–E directions are similar. The seiches generated by the wind pulse in D–F and F–D directions are also similar. In case E–C (Figure 10), the period of primary seiches in Dapeng Bay is about 3.5 h with an amplitude of about 17 cm. The general characteristics of primary seiches in Daya Bay are similar to those in Dapeng Bay in case E–C. The seiches generated by the wind pulse in the directions of E–C and C–E are very close to the free oscillations induced by Typhoon Mangkhut in terms of periods and amplitudes of primary seiches, due to the fact that the

wind directions associated with Typhoon Mangkhut in these two bays before the landfall were close to the E–C direction.

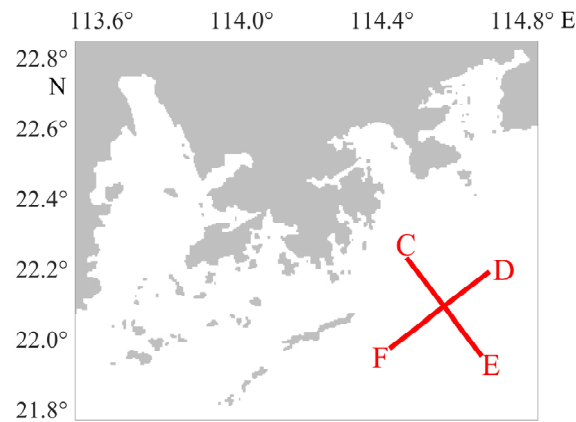


**Figure 9.** Four directions (D–F, E–C, F–D, and C–E) of constant wind fields used to drive the nested-grid modeling system.

**Table 2.** Directions and speeds of constant surface winds used in driving the nested-grid modeling system in each idealized experiment.

Idealized Run	Direction	U (m/s)	V (m/s)
1	D–F	–30	–20
2	E–C	–20	30
3	F–D	30	20
4	C–E	20	–30

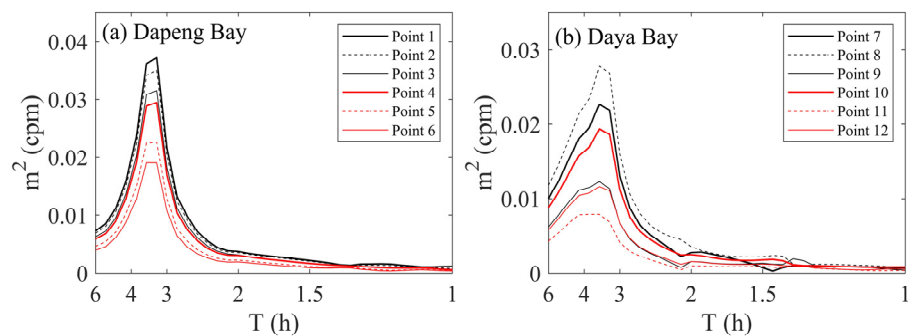


**Figure 10.** Power spectra of sea levels at (a) six locations in Dapeng Bay and (b) six locations in Daya Bay based on results produced by the inner sub-model with the direction of constant wind forcing in the E–C direction.

In comparison with the results in case E–C, seiches generated by the wind pulse in the D–F direction (Figure 11), have very small amplitudes, mainly because the wind directions in case D–F (or F–D) are normal roughly to the longitudinal axes of two bays and, therefore, the wind forcing is less effective at generating the significant coastal setup inside these two bays. In case D–F, the period of the primary seiches in Dapeng Bay is about 3.5 h; however, seiches with periods of 1.9 and 1.3 h are also present. In Daya Bay, in addition to the primary seiches with a period of about 4.0 h, seiches with periods of 2.0 and 1.4 h are also excited in case D–F. Based on the natural periods listed in Table 1, the seiches with a period of 1.3 h in Dapeng and Daya Bays can be either the second mode of seiches in a semi-closed channel of which the longitudinal axis is parallel to the bay mouth or the first mode of seiches in a closed channel of which the longitudinal axis is normal to the bay mouth.

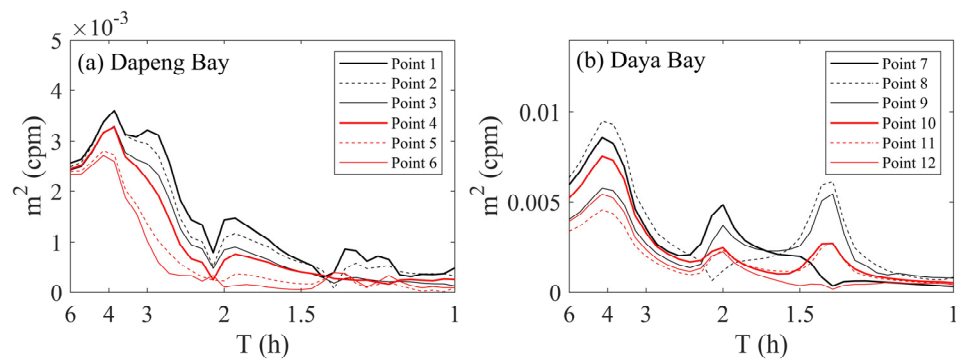


**Figure 11.** As in Figure 10 in (a) Dapeng Bay and (b) Daya Bay, except the direction of constant wind forcing is in the D–F direction.

Distributions of sea levels in Daya Bay after the wind pulse in the E–C (or E–C) direction have similar spatial features, but with different magnitudes, to the counterparts after Typhoon Mangkhut, namely, the first mode of seiches in a semi-closed channel. For the wind pulse in the F–D (D–F) direction (Figure 12), by comparison, the distributions of sea levels in Daya Bay differ significantly from the counterparts in case E–C. The sea levels in case F–D (Figure 12) have many small-scale features in Daya Bay, particularly with large free oscillations in Fanhe Harbor. At 00.00 (2 h after the end of the constant wind forcing), the sea levels in case F–D are positive and large, at about 30 cm, at the head of Fanhe Harbor and negative and large, at about –30 cm, near Aotou (Figure 12a). The sea levels at this time are relatively small near the mouth of Daya Bay. At 00:30, the sea levels are negative and large, at about –20 cm, at the head of Fanhe Harbor and positive and large, at about 35 cm, at Aotou (Figure 12b). At 01:00, the sea levels are about 15 cm at the head of Fanhe Harbor and relatively larger, at about 30 cm, over the area outside the harbor (Figure 12c), and large and positive over the central area of Daya Bay. At 1:30, the sea levels are significant and large, over 40 cm, at the head of Fanhe Harbor, and also positive and about 10 cm at Aotou (Figure 12d). At the subsequent times, the sea levels are relatively small but still have significant oscillations with large spatial variability (Figure 12e–i). Figure 12 demonstrates that free oscillations after the wind pulse in Daya Bay have seiches with periods of 1.3 and 1.4 h, in addition to the period of about 4.0 h. Oscillations with periods of 1.3 and 1.4 h are close to the first modes of seiches with periods of 0.9 and 1.3 h calculated using Merian’s formula for a narrow and closed channel. In addition, Figure 12 demonstrates that there is no second mode of seiches along the bay mouth direction, and only the first mode exists. This suggests that the two different periods of seiches in the F–D direction are the superposition of the first modes of seiches in two narrow channels in different orientations. In practice, due to the variation of the wind field and the irregularity of bay morphology, seiches with different directions and periods often coexist.

The model’s results in four idealized experiments demonstrate that storm-induced accumulation of water mass (or sea level setup) over different sides of a coastal bay generates different types of seiches, which can coexist in the bay. The model’s results also demonstrate that the amplitude of the first mode of seiches in the semi-closed narrow channel with its longitudinal axis normal to the bay mouth is larger than that in the closed narrow channel with the longitudinal axis parallel to the bay mouth. This is because it is easier for water mass to accumulate in the former case than in the latter case. In the latter case, water mass can directly enter or flow out, and the accumulation of water mass is smaller, leading to smaller seiche amplitudes than in the former case.

Typhoon Mawar made landfall over eastern Shenzhen. During its landing process, the wind directions associated with Mawar in Shenzhen are roughly in the D–F direction, i.e., in the direction parallel to the bay mouth, which is more likely to generate seiches with a period of about 1.2 h and seiches with a larger amplitude than that generated by Typhoon Mangkhut. The four idealized experiments clearly illustrate the influence of wind

directions on the characteristics of seiches and further demonstrate the influence of typhoon landing locations on seiches. Accurate wind forcing should enable us to generate realistic seiches associated with typhoons. One possible way to do this is to use an atmospheric model (such as WRF) coupled to our ocean circulation modeling system to get more realistic winds associated with typhoons. Our work in this area is in progress.

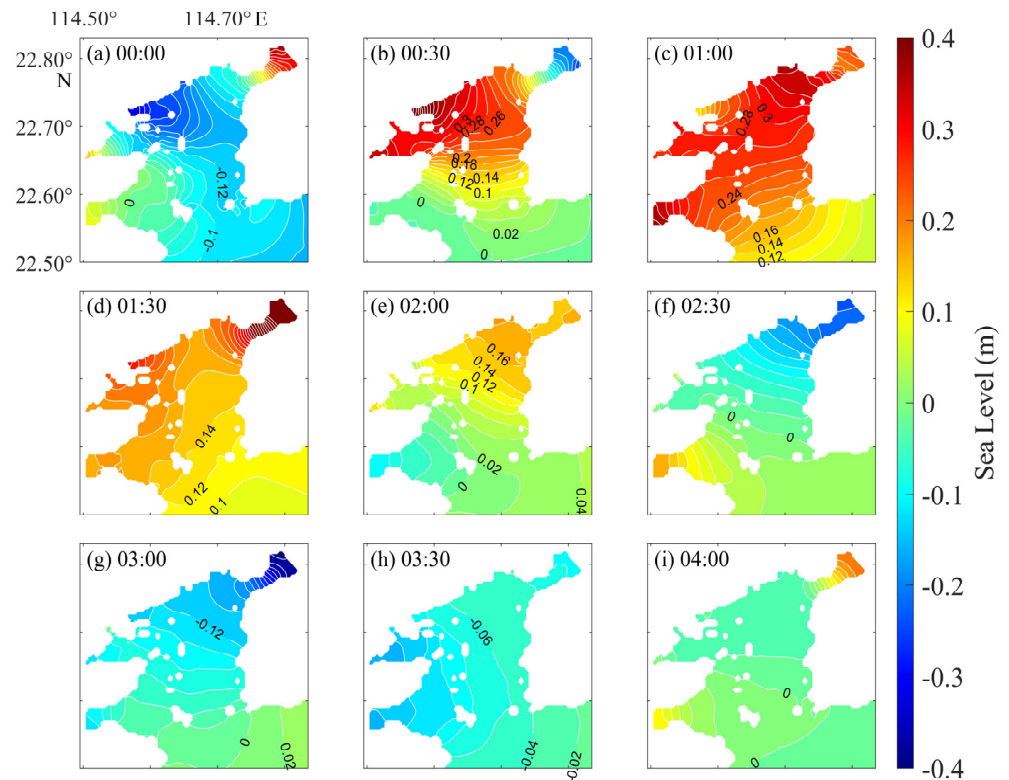


**Figure 12.** Distributions of instantaneous sea levels produced by the inner sub-model in Daya Bay after a wind pulse in the D–F direction at nine different times (a–i) between 00:00 (2 h after the end of the constant wind forcing) and 04:00.

### 5. Summary

Observations and model results were used in this study to investigate characteristics of seiches over the coastal waters off Shenzhen, China. The model results were generated by a nested-grid modeling system based on the Regional Ocean Modeling System. The nested-grid system consists of three sub-models: a course-resolution (~9 km) outer sub-model, an intermediate resolution (~1.8 km) middle model and a fine-resolution (~400 m) inner-model. The domain of the inner-most sub-model of the nested-grid system covers Dapeng Bay, Daya Bay and adjacent coastal waters off Shenzhen. The inner sub-model was found to perform very well in simulating tides and storm surges over coastal waters off Shenzhen.

Spectral analysis of sea-level observations demonstrated that, after the passage of Typhoon Mangkhut in September 2018, primary seiches had a period of about 3.8 h at station Nanao in Dapeng Bay and about 4.0 h at station Dongshan in Daya Bay. The estimated amplitude of the primary seiches was about 20 cm at Nanao and about 27 cm at Dongshan after Mangkhut. The primary seiches estimated from the spectral analysis of observed sea levels had a period of about 3.5 h at station Nanao in Dapeng Bay and about 4.0 h at station Dongshan in Daya Bay after the passage of Typhoon Mawar in September 2017. The estimated amplitude of the primary seiches after Mawar was about 19 cm at Nanao and about 30 cm at Dongshan. Seiches with a period of about 1.2 h and an amplitude of 20 cm also occurred at Dongshan after Mawar, which were larger than the counterparts after Typhoon Mangkhut.

The results produced by the inner model of the nested-grid modeling system were used to examine the main processes affecting the generations and propagations of seiches in Dapeng and Daya Bays after typhoons. The model's results demonstrated that the seiches after passages of Mawar and Mangkhut are oscillations excited by the relaxation of water accumulation caused by the wind stress, and those oscillations are the resonance motions of dynamically free waves.

The generation and propagation of seiches by wind-induced sea level perturbations in Daya Bay were further examined using model results in four idealized numerical experiments with a wind pulse with different wind directions. Analysis of the model's results from these experiments demonstrated that when the wind pulse causes the water body to accumulate on the sides of the bay, the primary oscillations in the bay are equivalent to seiches in a closed channel. On the other hand, when the wind pulse causes the water body to accumulate over the head of the bay, the primary oscillations in the bay are equivalent to seiches in a semi-closed channel. Typhoon landing locations lead to different wind directions in Shenzhen; therefore, typhoon landing locations have a direct impact on the type and characteristics of seiches. In future, more observations will progress understanding of this process in more detail. This phenomenon about varying periods of seiches due to different wind directions probably also exists in other coastal regions.

**Author Contributions:** Data curation, G.D.; Formal analysis, S.C.; Funding acquisition, G.D. and J.X.; Methodology, G.D. and J.X.; Project administration, J.X. and S.C.; Writing—original draft, G.D.; Writing—review & editing, J.X., J.S. and S.C. All authors have read and agreed to the published version of the manuscript.

**Funding:** This research was funded by the Shenzhen Peacock Plan, grant number KQJSCX20170720174016789, the Shenzhen University Sustainable Support Plan, grant number WDZC20200819105831001 and the Fund for Promoting High-Quality Economic Development in Guangdong Province (Marine Economic Development Project), grant number GDOE[2019]A45. Shengli Chen is supported by the Scientific Research Start-up Funds (QD2021021C). J.S. was also funded by NSERC, MEOPAR and OFI.

**Institutional Review Board Statement:** Not applicable.

**Informed Consent Statement:** Not applicable.

**Data Availability Statement:** The measurement data is archived by the Shenzhen Marine Monitoring and Forecasting Center.

**Acknowledgments:** The authors are grateful for support of measured data from Shenzhen Marine Monitoring and Forecasting Center.

**Conflicts of Interest:** The authors declare no conflict of interest.

## References

1. Rif'atin, H.Q.; Magdalena, I. Seiches in a Closed Basin of Various Geometric Shape. *J. Phys. Conf. Ser.* **2019**, *1245*, 012061. [[CrossRef](#)]
2. Rabinovich, A.B. Seiches and Harbor Oscillations. In *Handbook of Coastal and Ocean Engineering*; World Scientific: Singapore, 2009.
3. Wu, S.; Wang, X.; Dai, M. Primary Study on Characteristics and Formation Cause of Seiches in the Bays. *Mar. Sci. Bull.* **1999**, *18*, 6–12.
4. Li, K.; Wang, Y.; Huang, Y. The Seiche in Dapeng Bay. *J. Oceanogr. Huanghai Bohai Seas* **1990**, 11–15. Available online: <http://www.nmglib.com:8901/article/detail.aspx?id=288897> (accessed on 16 January 2022).
5. Kenney, B.C. Lake surface fluctuations and the mass flow through the narrows of Lake Winnipeg. *J. Geophys. Res. Ocean.* **1979**, *84*, 1225–1235. [[CrossRef](#)]
6. Chuang, W.S.; Boicourt, W.C. Resonant Seiche Motion in the Chesapeake Bay. *J. Geophys. Res. Ocean.* **1989**, *94*, 2105–2110. [[CrossRef](#)]
7. Bajo, M.; Međugorac, I.; Umgiesser, G.; Orlić, M. Storm Surge and Seiche Modelling in the Adriatic Sea and the Impact of Data Assimilation. *Q. J. R. Meteorol. Soc.* **2019**, *145*, 2070–2084. [[CrossRef](#)]
8. Gomis, D.; Monserrat, S.; Tintoré, J. Pressure-forced seiches of large amplitude in inlets of the Balearic Islands. *J. Geophys. Res.* **1993**, *98*, 14437–14445. [[CrossRef](#)]
9. Luettich, R.A.; Carr, S.D.; Reynolds-Fleming, J.V.; Fulcher, C.W.; McNinch, J.E. Semidiurnal seiching in a shallow, micro-tidal lagoonal estuary. *Cont. Shelf Res.* **2002**, *22*, 1669–1681. [[CrossRef](#)]

10. Lemon, D.D. Seiche Excitation in a Coastal Bay by Edge Waves Travelling on the Continental Shelf. Ph.D. Dissertation, University of British Columbia, Vancouver, BC, Canada, 1975.
11. Fan, G.; Xu, Y. Seiche Phenomenon and the Cause Analysis in the Sea Area of Laohutan of Dalian. *Trans. Oceanol. Limnol.* **2014**, *4*, 139–143.
12. Cao, C.; Guo, K.; Li, K.; Chen, Z. Synoptic analyses for the formation of large-amplitude seiche in the main harbors along the coasts of the Bohai Sea and the Huanghai Sea. *Acta Oceanol. Sin.* **2001**, *23*, 24–32.
13. Li, M.; Zhong, L.; Boicourt, W.C.; Zhang, S.; Zhang, D.L. Hurricane-induced storm surges, currents and destratification in a semi-enclosed bay. *Geophys. Res. Lett.* **2006**, *33*, L02604. [[CrossRef](#)]
14. Proudman, J. *Dynamical Oceanography*; Methuen: London, UK, 1953; pp. 85–89.
15. Raichlen, F. Harbor resonance. In *Estuary and Coastline Hydrodynamics*; Ippen, A.T., Ed.; McGraw Hill Book Comp.: New York, NY, USA, 1966; pp. 281–340.
16. Wu, Z.; Jiang, C.; Chen, J.; Long, Y.; Deng, B.; Liu, X. Three-Dimensional Temperature Field Change in the South China Sea during Typhoon Kai-Tak (1213) Based on a Fully Coupled Atmosphere–Wave–Ocean Model. *Water* **2019**, *11*, 140. [[CrossRef](#)]
17. Yuxing, W.; Ting, G.; Ning, J.; Zhenyu, H. Numerical Study of the Impacts of Typhoon Parameters on the Storm Surge Based on Hato Storm over the Pearl River Mouth, China. *Reg. Stud. Mar. Sci.* **2020**, *34*, 101061. [[CrossRef](#)]
18. Holland, G.J. An analytic model of the wind and pressure profiles in hurricanes. *Mon. Weather. Rev.* **1980**, *108*, 1212–1218. [[CrossRef](#)]
19. Ying, M.; Zhang, W.; Yu, H.; Lu, X.; Feng, J.; Fan, Y.; Zhu, Y.; Chen, D. An Overview of the China Meteorological Administration Tropical Cyclone Database. *J. Atmos. Ocean. Technol.* **2014**, *31*, 287–301. [[CrossRef](#)]
20. Lu, X.; Yu, H.; Ying, M.; Zhao, B.; Zhang, S.; Lin, L.; Bai, L.; Wan, R. Western North Pacific Tropical Cyclone Database Created by the China Meteorological Administration. *Adv. Atmos. Sci.* **2021**, *38*, 690–699. [[CrossRef](#)]
21. Egbert, G.D.; Erofeeva, S.Y. Efficient Inverse Modeling of Barotropic Ocean Tides. *J. Atmos. Ocean. Technol.* **2002**, *19*, 183–204. [[CrossRef](#)]